Applied Catalysis B: Environmental 148–149 (2014) 322–329

Contents lists available at ScienceDirect

Applied Catalysis B: Environmental

journal homepage: www.elsevier.com/locate/apcatb

Influence of alkaline and alkaline-earth cocations on the performance of Ni/β-SiC catalysts in the methane tri-reforming reaction

Jesús Manuel García-Vargas*, José Luis Valverde, Javier Díez, Paula Sánchez, Fernando Dorado

Departamento de Ingeniería Química, Facultad de Ciencias Químicas, Universidad de Castilla-La Mancha, Avenida Camilo José Cela 12, 13005 Ciudad Real, Spain

ARTICLE INFO

Article history:
Received 29 July 2013
Received in revised form 5 November 2013
Accepted 8 November 2013
Available online 18 November 2013

Keywords:
Tri-reforming
TPR
TPO
Nickel
Promoters

ABSTRACT

The influence of alkaline (Na, K) and alkaline earth (Mg, Ca) cocations on the behaviour of Ni/β-SiC catalyst for the tri-reforming of methane has been evaluated in this work. The cocations were loaded by co-impregnation with Ni, using different cocation/Ni ratios. Catalysts were characterized by AAS, TPR, N_2 adsorption, CO_2-TPD and XRD after calcination, as well as by XRD and TPO after reaction. It was analyzed the effect of the cocations on the β-SiC oxidation rate, which was increased when Na or K were loaded. The presence of Mg led to a high catalytic performance and stability (with a lower coke formation) since it provoked a decrease of Ni particle size and an increase of both the interaction between nickel and promoter and the catalyst basicity. Catalysts with Ni:Mg molar ratios of 2/1 and 1/1 showed the best performance in terms of activity and stability and formation of coke. These catalysts were considered good candidates for the tri-reforming of methane.

1. Introduction

Tri-reforming of methane is an interesting process, as production of synthesis gas from carbon dioxide and methane helps to resolve two main problems: first, these two gases have a well known green house effect, so that this reaction decreases their emission to the atmosphere; second, synthesis gas is the raw material for many chemical process, e.g. production of valuable chemical compounds through Fischer–Tropsch synthesis [1,2], dimethyl ether synthesis [3], or methanol production [4,5].

The goal of this process is to avoid the limitations related to each one of the three reforming reactions involved in this process: steam reforming (Eq. (1)), dry reforming (Eq. (2)), and partial oxidation of methane (Eq. (3)).

$$H_2O + CH_4 \rightarrow CO + 3H_2 \quad (\Delta H^\circ = 206.3\,kJ\,mol^{-1}) \tag{1}$$

$$CO_2 + CH_4 \rightarrow 2CO + 2H_2 \quad (\Delta H^\circ = 247.3\,kJ\,mol^{-1}) \tag{2}$$

$$CH_4 + (1/2)O_2 \rightarrow CO + 2H_2 \quad (\Delta H^\circ = -35.6\,kJ\,mol^{-1}) \tag{3}$$

The properties that make interesting methane tri-reforming are: a higher resistance against coke deactivation compared to dry reforming, due to the presence in the reaction environment of oxidants (H_2O and O_2) that could eliminate the coke previously generated (Eqs. (4)–(7)); it is less endothermic than dry or steam reforming as partial oxidation is very exothermic and mitigates the endothermicity of the other two processes; and finally the H_2/CO molar ratio could be controlled by modifying the reagents ratio, yielding a synthesis gas with a H_2/CO molar ratio around 2.

$$2CO \rightleftarrows C + CO_2 \quad (\Delta H^\circ = -172.2\,kJ\,mol^{-1}) \tag{4}$$

$$CH_4 \rightleftarrows C + 2H_2 \quad (\Delta H^\circ = 74.9\,kJ\,mol^{-1}) \tag{5}$$

$$C + H_2O \rightleftarrows CO + H_2 \quad (\Delta H^\circ = 131.4\,kJ\,mol^{-1}) \tag{6}$$

$$C + O_2 \rightleftarrows CO_2 \quad (\Delta H^\circ = -393.7\,kJ\,mol^{-1}) \tag{7}$$

Nickel has been selected as the active phase for different reforming reactions by many authors [6–9] due to its low cost compared to other metals and its high activity. Silicon carbide exhibits a high thermal conductivity, a high resistance towards oxidation, a high mechanical strength, chemical inertness and average surface area (around 25 $m^2\,g^{-1}$). Therefore, it is a good candidate as a catalyst support [9]. Silicon carbide has been chosen as a support for steam reforming by some authors. The known high thermal conductivity of this material may be interesting in order to improve the temperature profile of the catalyst bed and decrease the temperature

* Corresponding author. Tel.: +34 926295300; fax: +34 926295256.
E-mail address: JesusManuel.Garcia@uclm.es (J.M. García-Vargas).

0926-3373/$ – see front matter © 2013 Elsevier B.V. All rights reserved.
http://dx.doi.org/10.1016/j.apcatb.2013.11.013

differences that the high endothermicity of this reaction can originate in the catalyst bed [10]. In addition, many other works have shown that this material has interesting properties as catalytic support for different reforming reactions [11,12]. In this work, nickel catalysts supported over β-SiC, have been prepared. This kind of catalysts has shown acceptable performance for the tri-reforming process in previous works [13,14]. Nevertheless, it is necessary to improve the catalytic stability, specially its resistance against coke deactivation.

Alkaline and alkaline earth oxides have been extensively studied as traditional promoters for heterogeneous catalysts, as they are easily accessible and have a low cost. J. Juan-Juan et al. [15] studied the influence of K load in Ni/Al_2O_3 catalyst for dry reforming of methane, reporting that the presence of potassium in Ni/Al_2O_3 catalysts hinders the accumulation of coke on the catalyst surface during the dry reforming of methane, but produces a decrease in the catalytic activity. The addition of Na as promoter in Co/ZnO catalysts for steam reforming was analyzed by A. Casanovas et al. [16] and was compared with the effect of other metals, seeing that Na promoted catalysts have a higher activity and selectivity towards reforming products than the original Co/ZnO catalyst. Alkaline earth metals have also been extensively studied as catalyst promoters for different reforming reactions. It was reported that MgO-CaO mixed oxide was an excellent support: carbon deposition was effectively prevented during the reaction of CO_2 with CH_4 by supporting Ni on it [17]. The suppression of carbon deposition was attributed to the basicity of the MgO-CaO mixed oxide. Other authors have suggested that carbon deposition is suppressed when the metal is supported on a metal oxide with strong Lewis basicity [18,19]. Then, the higher the support Lewis basicity, the higher the ability of the catalyst to chemisorb CO_2 [20]. A higher concentration of adsorbed CO_2 is suggested to reduce carbon formation via CO disproportionation (Eq. (4)) by shifting the equilibrium concentrations. However, Zhang and Verykios reported that the addition of a basic CaO promoter to $Ni/\gamma\text{-}Al_2O_3$ increased both catalyst stability and carbon deposition in the form of Ni carbide and/or graphitic carbon, enhancing the reactivity of these species [18]. In addition, X-ray photoelectron spectroscopy (XPS) results by Tang et al. [21] also illustrated that the addition of either MgO or CaO to $Ni/\alpha\text{-}Al_2O_3$ greatly increased both catalyst basicity and carbon deposition during CO_2 reforming of CH_4. In this work, we report the influence of these traditional promoters over Ni/β-SiC catalysts and how these promoters modified its catalytic performance for the tri-reforming process.

2. Experimental

2.1. Catalyst preparation

Nickel-supported catalysts were prepared by the impregnation method using nickel nitrate $Ni(NO_3)_2{\cdot}6H_2O$ (PANREAC). The support used was β-SiC, provided by SICAT CATALYST. Na, K, Mg and Ca, used as promoters, were also added to the catalyst by the impregnation method. This way a solution of nickel nitrate and the corresponding metal hydroxide, with the required quantity to obtain a 5 wt% Ni catalyst and the Ni:M (M = Na, K, Mg or Ca) molar ratio desired, was prepared. In the first part of the study, eight catalysts were prepared with a Ni:M molar ratio fixed at 10/1 and 2/1 for each metal. For a comparison purpose, a Ni/β-SiC catalyst without any promoter was also prepared. In the last part of the study, Mg was selected as promoter. This way, two catalysts were prepared in order to complete the present study with a Ni:Mg molar ratio fixed at 4/1 and 1/1. All the catalysts prepared in this work were dehydrated at 393 K for 12 h and subsequently calcined in air at 1173 K for 2 h.

2.2. Catalyst characterization

Ni and Na, K, Mg or Ca metal loading were determined by atomic absorption (AA) spectrophotometry, using a SPECTRA 220FS analyzer. Samples (ca. 0.5 g) were treated in 2 mL HCl, 3 mL HF and 2 mL H_2O_2 followed by microwave digestion (523 K). In order to calculate textural properties (surface area and total pore volume) samples were outgassed at 453 K under vacuum for 12 h and analyzed afterwards in a QUADRASORB 3SI sorptometer apparatus with N_2 as the sorbate at 77 K. Temperature-programmed reduction (TPR) experiments were conducted in a commercial Micromeritics AutoChem 2950 HP unit with TCD detection. Samples (ca. 0.15 g) were loaded into a U-shaped tube and ramped from room temperature to 1173 K ($10\,K\,min^{-1}$), using a reducing gas mixture of 17.5% (v/v) H_2/Ar ($60\,cm^3\,min^{-1}$). CO_2 temperature-programmed desorption (TPD) experiments were also conducted in the Micromeritics AutoChem 2950 HP unit. The sample (0.15 g) was loaded in a quartz tube, reduced and pretreated. Then, a flow of $30\,mL\,min^{-1}$ of CO_2 (99.99% purity, Praxair certified) was passed through the sample for 30 min at a constant temperature of 313 K. Finally, the physically adsorbed carbon dioxide was removed by a flow of He for another 30 min. The sample was then heated in $50\,mL\,min^{-1}$ of He with a heating rate of $10\,K\,min^{-1}$ up to 1273 K. XRD analyses were conducted with a Philips X'Pert instrument using nickel-filtered Cu Kα radiation. The samples were scanned at a rate of $0.02^\circ\,step^{-1}$ over the range $5^\circ \leq 2\theta \leq 90^\circ$ (scan time = 2 s $step^{-1}$). Temperature-programmed oxidation (TPO) analyses were performed in the Micromeritics AutoChem 2950 HP unit, flowing $50\,cm^3\,min^{-1}$ of pure oxygen from room temperature to 1173 K ($10\,K\,min^{-1}$).

2.3. Catalyst activity measurements

The catalytic behaviour was tested in a tubular quartz reactor (45 cm long and 1 cm internal diameter). The catalyst was placed on a fritted quartz plate located at the end of the reactor. The reactor was heated with a furnace (Lenton) and the temperature measured with a K-type thermocouple (Thermocoax). Reaction gases were Praxair certified standards of CH_4 (99.995% purity), 10% CO_2/N_2, O_2 (99.99% purity), and N_2 (99.999% purity). The water content in the reaction mixture was controlled using the vapour pressure of H_2O at the temperature of the saturator (24 °C). The temperature of the saturator was controlled by a heating bath. All lines placed downstream from the saturator were heated above 373 K to prevent condensation. The saturation of the feed stream by water at the working temperature was verified by a blank experiment in which the amount of water trapped by a condenser was measured for a specific time and compared with the theoretical value. The feed composition (by volume %) was as follows: 6% CH_4, 3% CO_2, 3% H_2O, 0.6% O_2, N_2 balance, with a total flow of $100\,NmL\,min^{-1}$. This composition was used in previous studies [13,22,23] to get a molar ratio in the feed of $CH_4/CO_2/H_2O/O_2 = 1/0.5/0.5/0.1$. In a previous work [14] we observed that with this composition we could obtain a synthesis gas with a H_2/CO molar ratio close to the desired ratio for most of the synthesis gas applications ($H_2/CO = 2$). The weight hourly space velocity (WHSV) of the total gas mixture was fixed at $60{,}000\,NmL\,h^{-1}\,g^{-1}$. The catalytic activity was evaluated at 1073 K and atmospheric pressure for 24 h. Gas effluents were analyzed with a micro gas chromatograph (Varian CP-4900). Methane and carbon dioxide consumption rates were calculated as follows: [inlet molar flow of CH_4/CO_2 – outlet molar flow of CH_4/CO_2]/nickel weight. A blank experiment carried out with pure SiC showed no appreciable conversion in the considered conditions.

3. Results and discussion

3.1. Catalyst characterization

As commented above, the first part of the study corresponds to an evaluation of four different cocations (Na, K, Mg and Ca) loaded as promoters in Ni/β-SiC catalysts for methane tri-reforming. They were prepared with a M/Ni molar ratio of 1/10 and 1/2, where M represents the cocation. These catalysts were characterized by atomic absorption spectrophotometry, XRD, TPR, N_2 adsorption and CO_2-TPD analysis. The main results are listed in Table 1. Fig. 1 shows the diffraction spectrum for the parent β-SiC used as support (Fig. 1a), and those obtained for catalysts Ni:Na = 2/1, Ni:K = 2/1, Ni, Ni:Na = 10/1 and Ni:K = 10/1, before and after reduction (Fig. 1b–f). The addition of Ni did not significantly alter the β-SiC structure. Only minor changes due to the presence of NiO or Ni peaks were observed. Fig. 1b, c, e and f, where the diagrams for the catalysts containing Na and K are represented, show that these two alkaline metals clearly attack the structure of β-SiC. For both promoters, a clear transition from β-SiC to α-cristobalite, a high-temperature polymorph of SiO_2, is observed when a high amount of promoter is introduced. Thus, the principal diffraction peak, and many others, corresponds to one of the α-cristobalite reflections (Fig. 1b and c). The transient from β-SiC to α-cristobalite is an oxidation process that probably occurs during the calcination of the catalysts. Na and K have been reported to be poisons for SiC that make it more easily oxidable. Pareek and co-workers [24] attributed this SiC oxidation rate enhancement to the capacity of the alkali compounds to get dissolved in the SiO_2 and enhance the O_2 transport to the bulk SiC, leading to a drastically increased oxidation. Riley [25] also reported the effect of alkali environments on SiC, indicating that its oxidation is dramatically accelerated at high temperatures. However, he observed that SiC is not very affected by alkalis at temperatures under 1200 K. It is interesting to note that for the catalysts prepared with K as promoter, the peaks usually assigned to NiO or Ni could not be observed, even though the presence of this metal was confirmed by atomic absorption (Table 1). XRD diagrams showed that for the Na and K promoted catalysts there are some differences depending on the promoter load, as the relative intensity of the main α-cristobalite peak compared with the intensity of the principal β-SiC peak is clearly higher for high promoter loads. This means that the quantity of α-cristobalite species, and therefore the extension of the β-SiC oxidation, is higher for high promoter loads.

Fig. 2 shows the XRD results for the catalysts prepared using Mg or Ca as promoters. For both catalysts, Ni:Mg = 10/1 (Fig. 2c) and Ni:Mg = 2/1 (Fig. 2a), only the peaks attributed to β-SiC, NiO or Ni could be clearly assigned. For the catalyst Ni:Ca = 2/1, there are three peaks that cannot be assigned to the previously commented species. This fact could indicate the most probable presence of quartz in the sample, caused by an increase in the oxidation rate of β-SiC during the calcination step. This increase could be due to the presence of a relatively high content of Ca in the catalyst. This element has been pointed to decrease the stability against oxidation of SiC, despite it is less deleterious than alkali salts [26]. For the catalyst with a lower Ca loading, Ni:Ca = 10/1, the peaks likely related to quartz were not observed. Taking into account the calcination temperature (1173 K), SiC should be oxidized into amorphous SiO_2 or quartz [27]. However, this was not observed for Na and K promoted catalysts. They showed α-cristobalite as the main SiO_2 phase, which should be obtained at higher calcination temperatures [27]. However, Na [28] and K [24] induce crystallization of the amorphous silica into α-cristobalite at temperatures far below the normal transition temperature. In addition, the acid SiO_2, which forms the passive film that protects SiC from oxidation, will react in a higher extension with the more basic oxides [29], leading to a higher extension of the SiC oxidation.

Table 1
Main physical properties of the catalysts.

	Ni	Ni:Na 10/1	Ni:Na 2/1	Ni:K 10/1	Ni:K 2/1	Ni:Ca 10/1	Ni:Ca 2/1	Ni:Mg 10/1	Ni:Mg 4/1	Ni:Mg 2/1	Ni:Mg 1/1
Ni loading (%)	4.5	4.8	4.9	4.7	4.5	4.6	4.6	5.2	5.1	4.6	5.5
Surface area ($m^2\,g^{-1}$)	24.0	5.5	0.9	4.7	1.5	18.5	11.8	22.5	21.8	18.0	21.2
Total pore volume ($\times 10^2\,cm^3\,g^{-1}$)	14.4	3.6	1.1	2.9	0.8	12.9	8.3	13.1	14.0	11.2	12.6
Ni particle diameter from XRD (nm)	63	41	85	–	–	56	53	39	38	33	32
H_2 consumption ($mmol\,g^{-1}$)	0.896	0.542	0.378	0.284	0.198	0.761	0.556	0.873	0.623	0.615	0.553
Total basic sites ($\mu mol\,g^{-1}$)	5.46	–	–	–	–	5.63	2.82	11.05	11.84	13.54	14.39
Diffraction angle of NiO, 2θ	43.22	–	–	–	–	–	–	43.14	42.9	43.02	42.9

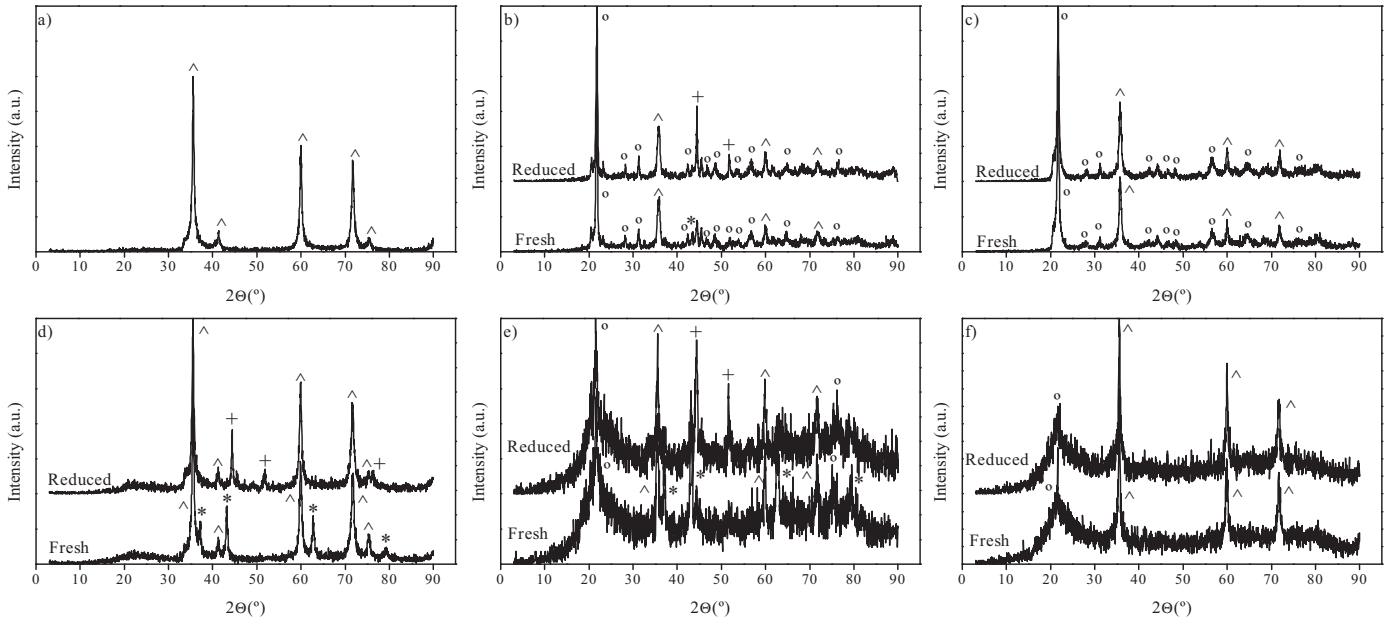

Fig. 1. XRD profiles of (a) catalyst support, (b) Ni:Na = 2/1, (c) Ni:K = 2/1, (d) Ni/β-SiC, (e) Ni:Na = 10/1 and (f) Ni:K = 10/1, where (^) denotes reflection of β-SiC, (+) denotes reflection of metallic nickel, (*) denotes reflection of nickel oxide and (◦) denotes reflection of α-cristobalite.

In order to analyze the influence of the promoters on the metal support interactions and reducibility of the catalysts, TPR experiments were carried out from room temperature to 1173 K. The corresponding data, represented in Fig. 3, showed several differences between the reference catalyst (Ni/β-SiC) and those ones that incorporated any promoter. Metal support interaction always increased after adding the promoter, shifting the reduction peaks towards higher temperatures. Among the samples prepared with Na or K as cocations (Fig. 3a), only catalyst Ni:Na = 10/1 showed a clear reduction peak. The profiles for the other samples were broad and small. The H_2 consumption during these TPR experiments (Table 1) also showed that Ni was hardly reduced. Regarding Ca and Mg promoted catalysts (Fig. 3b), sample Ni:Ca = 2/1 gave a similar response as those catalysts loaded with Na or K, being the H_2 consumption also too low. It can be noted a relation between the β-SiC oxidation reported from the XRD experiments and the low extent of Ni reduction. Thus, the oxidation process undergone by β-SiC and the consequent crystallization of SiO_2 made a big part of the Ni to be inaccessible by H_2. The TPR profile for sample Ni:Ca = 10/1 showed just one relatively sharp reduction

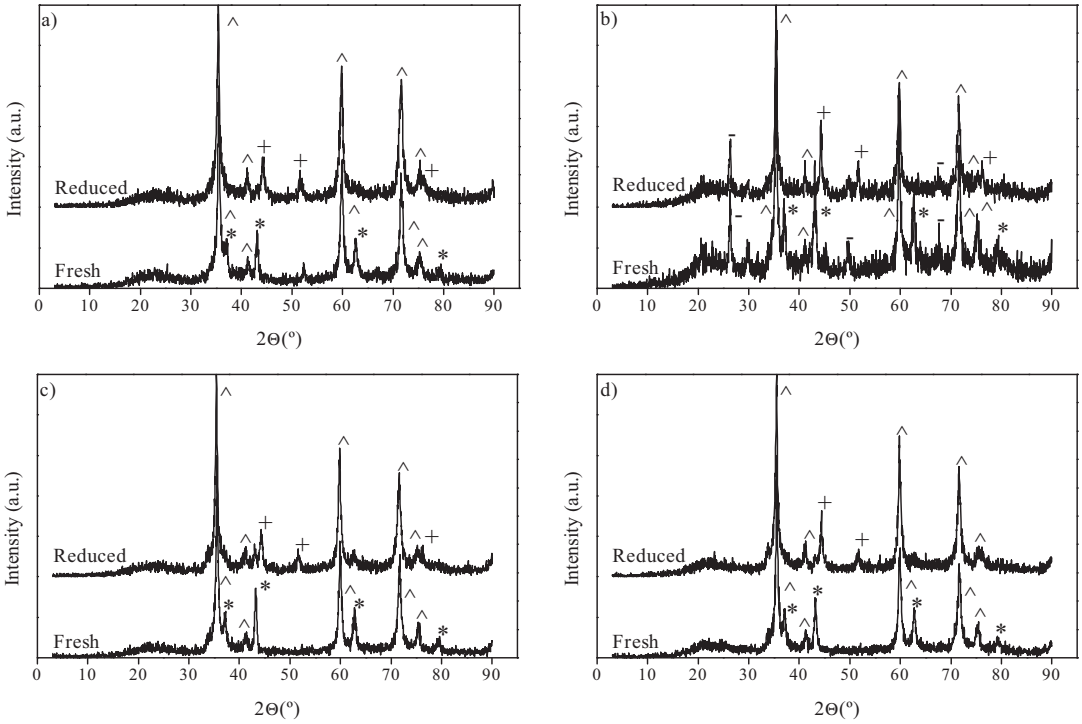

Fig. 2. XRD profiles (a) Ni:Mg = 2/1, (b) Ni:Ca = 2/1, (c) Ni:Mg = 10/1 and (d) Ni:Ca = 10/1, where (^) denotes reflection of β-SiC, (+) denotes reflection of metallic nickel, (*) denotes reflection of nickel oxide and (−) denotes reflection of quartz.

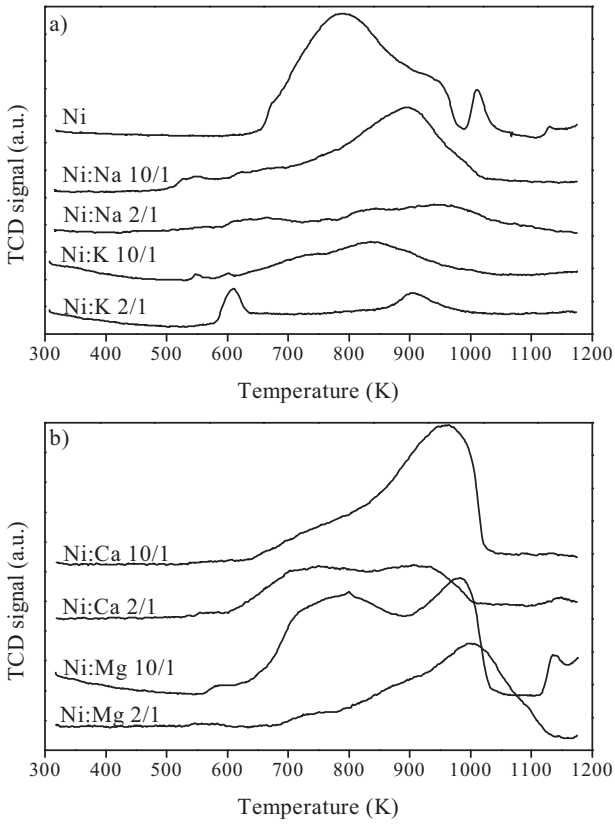

Fig. 3. TPR profiles: (a) Reference, Na and K promoted catalysts; (b) Mg and Ca promoted catalysts.

peak around 950 K. Comparing this profile with that of Ni/β-SiC, it seems that the presence of a low amount of Ca increased the metal support interaction. For the reference catalyst, it was obtained a profile with two overlapped peaks with maxima around 720 and 870 K, followed by a small peak obtained at 1140 K. The peak at low temperature is usually attributed to the reduction of bulk NiO, while peaks at higher temperatures are attributed to a higher interaction between nickel and support, originating nickel silicate [30,31]. It can be observed that the addition of low quantities of Mg increased the Ni dispersion and decreases the H_2 consumption during the TPR experiments (Table 1). The presence of Mg in catalysts Ni:Mg = 10/1 and Ni:Mg = 2/1 led to a shift of the reduction peaks towards higher temperatures, which was influenced by the Mg loading. The TPR corresponding to the catalyst with the lowest quantity of Mg, Ni:Mg = 10/1, showed two main reduction peaks at 750 and 980 K. The first peak could be related to the reduction of bulk NiO, as discussed for catalyst Ni/β-SiC, while the second one seems to correspond to the reduction of a NiO-MgO solid solution, as high calcination temperature usually leads towards the formation of this phase in catalysts where Ni and Mg are present, requiring higher reduction temperatures due to the strong interaction between NiO and MgO [32,33]. Comparing this catalyst with the reference, it is clear that the addition of this low amount of Mg increased the quantity of species hardly reducible and decreased the total amount of bulk NiO. Similarly, TPR profile for catalyst Ni:Mg = 2/1 showed that a higher quantity of Mg almost caused the peak assigned to the reduction of bulk NiO to disappear and led to an increase of the size of the peak assigned to the reduction of the NiO-MgO solid solution, which implied a decrease in the reducibility of NiO. Nickel particle size, surface area and basicity, in terms of CO_2 desorbed in a CO_2-TPD experiment, are also listed in Table 1. Ni particle size was obtained with the Debye–Scherrer equation using the data from the XRD patterns (1 1 1 reflection of Ni^0). This is not a very accurate method in order to obtain the actual metal particle size, but it could be applied in order to analyze different catalysts and get a relative comparison of the metal particle size. As a general trend, it could be observed a decrease in the Ni metal particle size after the promoter addition. However, it can be seen that the catalyst prepared with the highest quantity of Na shows the bigger particle size. It is likely related to the previously commented change in the support structure due to the enhance oxidation of SiC during the calcination. It leads to the formation of α-cristobalite, which is a compound with a high crystallinity and a very low surface area, facilitating the sintering of Ni particles during the calcination. It can be noted that presence of Ca did not greatly affect to Ni particle size. On the contrary, Mg promoted catalysts presented a lower Ni particle size than that of catalyst Ni/β-SiC. As it can be observed in Table 1, surface area and total pore volume values were in agreement with the XRD diagrams, being the surface area of the Na, K and Ca promoted catalysts much lower than that of the Mg promoted and reference catalysts, as a consequence of the increased oxidation rate of the former catalysts during the calcination and the changes in the support structure. The presence of Mg as promoter has a clear effect on the catalyst basicity, even for the catalyst with the lower Mg loading, increasing the basicity of the catalyst with the Mg content. However, Ca promoted catalyst did not show the same trend, having the catalyst with the highest quantity of Ca the lowest basicity, which seems to be related to the formation of quartz observed for this catalyst.

3.2. Catalytic activity

Taking into account the catalyst characterization results above discussed, only catalysts Ni:Ca = 10/1, Ni:Mg = 10/1 and Ni:Mg = 2/1 were considered to be tested for the methane tri-reforming process, being their catalytic performance compared to that of sample Ni/β-SiC. Catalytic results are plotted in Fig. 4. It could be seen that during the 24 h experiment the methane reaction rate of catalyst Ni/β-SiC (Fig. 4a) drops from 8.8×10^{-4} to 7.5×10^{-4} mol s^{-1} $g_{Ni}{}^{-1}$ (14.8% less after 24 h). Activity loss for sample Ni:Ca = 10/1 (Fig. 4b) was lower (from 7.9×10^{-4} to 7.3×10^{-4} mol s^{-1} $g_{Ni}{}^{-1}$, that is 7.6% less), being its methane reaction rate quite close to that of the reference catalyst. However, its carbon dioxide reaction rate was clearly lower, reaching values near to 0, thus yielding a H_2/CO molar ratio ranging from 2.5 to 2.9 (close to the stoichiometric value of the synthesis gas produced by the steam reforming reaction). Regarding catalysts Ni:Mg = 10/1 (Fig. 4c) and Ni:Mg = 2/1 (Fig. 4d), methane reaction rate was higher than that of the reference catalyst. The activity drop after 24 h was also clearly lower (2.6% and 1.1%, respectively). Hence, it could be drawn that the addition of Ca or Mg decreased, or at least did not increase, the carbon dioxide reaction rate. This is something unexpected as both promoters increased catalyst basicity, which has been often reported as a positive factor in dry reforming due to the higher CO_2 adsorption capacity of the catalyst [20]. Nevertheless, despite this general rule, it can be seen in Table 1 that the low quantity of Ca in catalyst Ni:Ca = 10/1 did not increase its basicity (compared to Ni/β-SiC).

On the other hand, catalysts containing Ca have been reported to shift the water gas shift equilibrium towards the formation of CO_2 at a temperature close to that selected in this work [34,35]. This process could be responsible of the carbon dioxide conversion decrease. Catalysts prepared with Mg as the promoter showed a higher CO_2 adsorption capacity than that of the reference catalyst (Table 1). Thus, it can be concluded that the presence of Mg increased the basicity of the catalyst. Anyway, as previously commented, catalysts Ni:Mg = 10/1 and Ni:Mg = 2/1 showed a similar CO_2 reaction rate and a lower CO_2 reaction rate, respectively, if

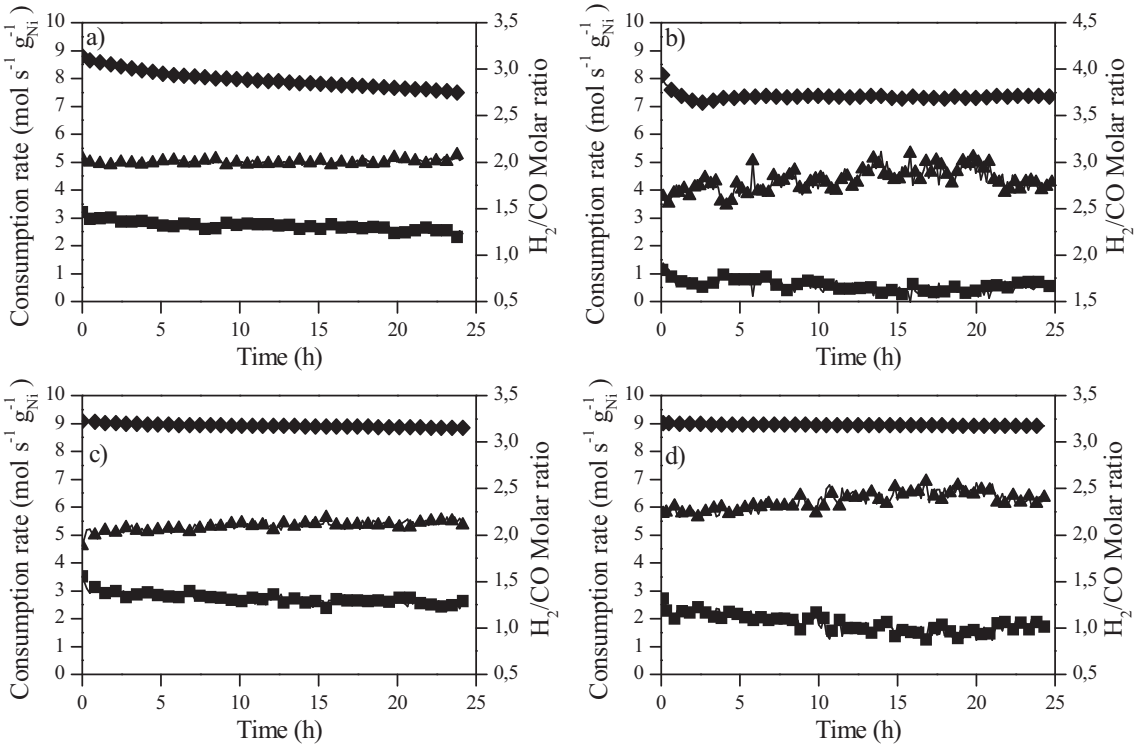

Fig. 4. Catalytic activity at 1073 K for (a) Ni/β-SiC, (b) Ni:Ca = 10/1, (c) Ni:Mg = 10/1 and (d) Ni:Mg = 2/1. Reaction conditions: CH_4 = 6%, CO_2 = 3%, H_2O = 3%, O_2 = 0.6%, N_2 balance, total flow rate = 100 NmL min^{-1}. CH_4 (♦) and CO_2 (■) consumption rates vs. time on stream (left axis), and H_2/CO molar ratio (▲) vs. time on stream (right axis).

compared as that of the reference sample, despite having a higher basicity. A higher basicity implies a higher CO_2 adsorption capacity of the catalyst, which usually is correlated to a higher reactivity of this molecule. However, these catalysts did not follow this trend. This behaviour will be deeply explained in the next section.

3.3. Influence of the Mg/Ni molar ratio

In order to better understand the influence of the Ni:Mg molar ratio on the catalytic performance in the tri-reforming process, other two catalysts were prepared with Ni:Mg molar ratios of 4/1 and 1/1. The same characterization techniques, previously commented, were applied to these catalysts. Fig. 5 shows the reduction profile for all the samples with Mg as promoter. The addition of Mg increased the temperature of the reduction peaks, which could be related to the occurrence of a higher interaction between NiO and MgO. A reduction profile evolution was observed as a function of Mg content. Thus, catalyst Ni/β-SiC showed at least two peaks overlapped with maxima around 720 and 870 K, followed by a small peak obtained at 1140 K, whereas catalyst Ni:Mg = 1/1, with the highest Mg content, showed a reduction peak with maximum at 1020 K. The higher the Mg content in the catalyst, the lower the catalyst reducibility was obtained. The presence of the peak at a high temperature would indicate that Ni and Mg were in the form of a NiO-MgO solid solution [32,33]. Bradord et al. [36] attributed the formation of this solid solution to the fact that Ni and Mg almost perfectly fit the Hume-Rothery criteria for the formation of an extensive solid solution, i.e., both cations have similar ionic radii, ca. 0.78 Å [37], the same common oxidation state (2^+), and the same bulk oxide structure, NaCl-type [38]. The formation of this NiO-MgO solid solution was also confirmed with the XRD experiments. The diffraction angle of NiO for the different Mg promoted catalysts is given in Table 1, showing a light decrease in this value with the Mg loading. This decrease in the diffraction angle of NiO in catalysts where there is Mg is usually attributed to the formation of a NiO-MgO solid solution [39,40].

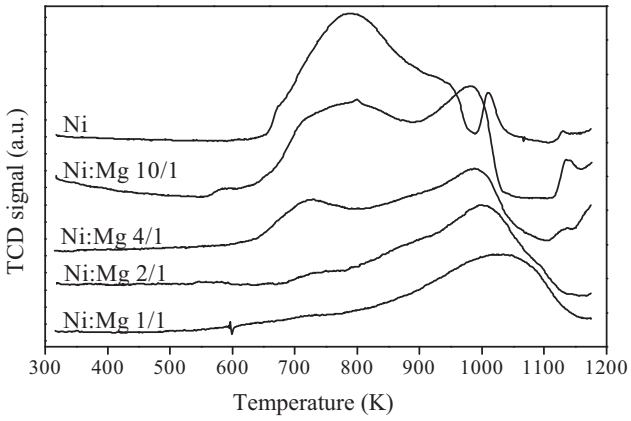

Fig. 5. TPR profiles for Mg promoted and Ni/β-SiC catalysts.

Particle size, surface area, total pore volume and catalysts basicity were also measured for these samples (Table 1). As previously commented, Ni:Mg catalysts showed a lower Ni particle size (compared with the reference sample). The results indicate that the higher the Mg loading, the lower the Ni particle size was obtained. Basicity of the catalysts also increased after the addition of Mg. The following order was established: Ni/β-SiC ≪ Ni:Mg = 10/1 ≅ Ni:Mg = 4/1 < Ni:Mg = 2/1 < Ni:Mg = 1/1.

The influence of the Mg loading on the catalytic performance of these catalysts was also studied. Fig. 6 shows for catalysts Ni:Mg = 4/1 and Ni:Mg = 1/1 the evolution of CH_4 reaction rate, CO_2 reaction rate and H_2/CO molar ratio during the 24 h tri-reforming tests. H_2/CO molar ratio is a key parameter in order to evaluate the catalytic performance in the tri-reforming process, as not only will determine the possible applications of the synthesis gas obtained but also indicates the relative importance of each reaction in the

Table 2
Reaction and characterization parameters after reaction.

	Ni	Ni:Mg 10/1	Ni:Mg 4/1	Ni:Mg 2/1	Ni:Mg 1/1
Average CH_4 reaction rate ($\times 10^4$ mol s^{-1} g_{Ni}^{-1})	7.96	8.92	8.46	8.95	8.65
Average CH_4 conversion (%)	73.7	95.4	88.8	84.7	97.9
Drop in CH_4 reaction rate (%)	14.8	2.6	2.3	1.1	0.9
Average CO_2 reaction rate ($\times 10^4$ mol s^{-1} g_{Ni}^{-1})	2.72	2.72	2.38	1.83	1.84
Average CO_2 conversion (%)	52.3	60.4	51.9	36.0	43.2
Drop in CO_2 reaction rate (%)	23.75	14.6	15.1	24.2	24.4
Average H_2/CO molar ratio	2.00	2.09	2.23	2.36	2.76
Oxygen consumption in TPO (mmol g^{-1})	35.28	10.70	8.23	5.71	6.24
Particle diameter from XRD after reaction (nm)	54	42	38	39	34

tri-reforming. Thereby, when the dry reforming activity is higher, the H_2/CO molar ratio obtained from global tri-reforming will be lower due to the stoichiometry of the dry reforming reaction (Eq. (2)). Catalytic deactivation in these catalysts was also lower than observed for the reference one, with a drop in the CH_4 reaction rate after 24 h of 2.3% for Ni:Mg = 4/1 and 0.9% for Ni:Mg = 1/1. Similarly, the CO_2 reaction rate was lower and the H_2/CO molar ratio higher in the Mg loaded catalysts than those corresponding to catalyst Ni/β-SiC. A comparison between the most representative reaction parameters for the different Mg promoted catalysts and the reference one is seen in Table 2. Mg promoted catalysts led to values of methane reaction rate and stability higher than those corresponding to catalyst Ni/β-SiC, indicating that this cocation had a beneficial effect over the methane tri-reforming. The best performance was found for samples Ni:Mg = 2/1 and Ni:Mg = 1/1,

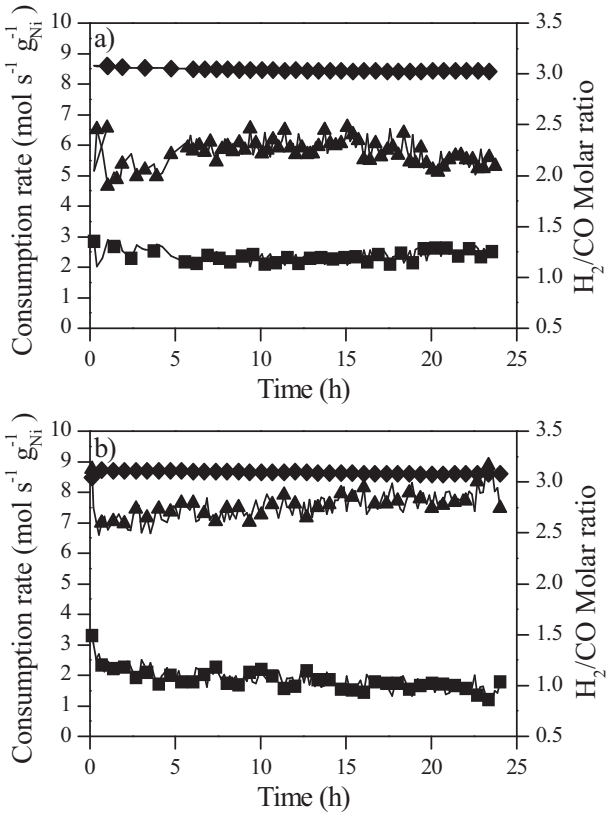

Fig. 6. Catalytic activity at 1073 K for (a) Ni:Mg = 4/1 and (b) Ni:Mg = 1/1. Reaction conditions: CH_4 = 6%, CO_2 = 3%, H_2O = 3%, O_2 = 0.6%, N_2 balance, total flow rate = 100 mL min^{-1}. CH_4 (♦) and CO_2 (■) consumption rates vs. time on stream (left axis), and H_2/CO molar ratio (■) vs. time on stream (right axis).

which showed very close catalytic results, with the highest CH_4 rate and a very high stability. It is also remarkable to note that the addition of Mg increased the H_2/CO molar ratio, which could be related to the high strength of the catalyst basic sites. Thus, L. Pino et al. [41] reported for Ni–La–CeO_2 catalysts an increase in the H_2/CO molar ratio, which was related to the higher concentration of strong basic sites with increasing La loads. The basic sites strengthening in our catalysts can be clearly seen in Fig. 7. The Mg addition led to an increase of the CO_2 desorption peak at ≈1075 K, which corresponded to the presence of very strong basic sites. Moreover, as above mentioned, an increase in the Mg loading made catalyst reduction to be more difficult. Hence, the higher the Mg loading, the higher the amount of NiO species present on the catalytic surface. In addition, NiO could act as a promoter of the water gas shift reaction. It has been reported that this oxide enhances the formation of surface oxygen intermediates such as $Ni(OH)_2$ and NiOOH [42], which would in turn lead to a lower CO_2 reaction rate.

Catalysts deactivation was evaluated in terms of the oxygen consumption of the coke generated after tri-reforming reaction tests in a TPO experiment. Fig. 8 shows the TPO profiles obtained. Table 2 lists the values of oxygen consumption in the TPO runs. It can be observed that the total amount of coke deposited onto the catalysts decreased with increasing values of the Mg loading, probably

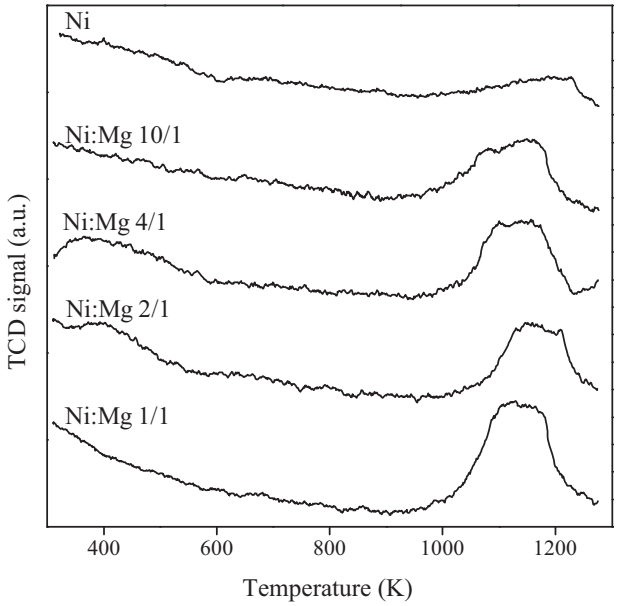

Fig. 7. CO_2-TPD profiles for Mg promoted and Ni/β-SiC catalysts.

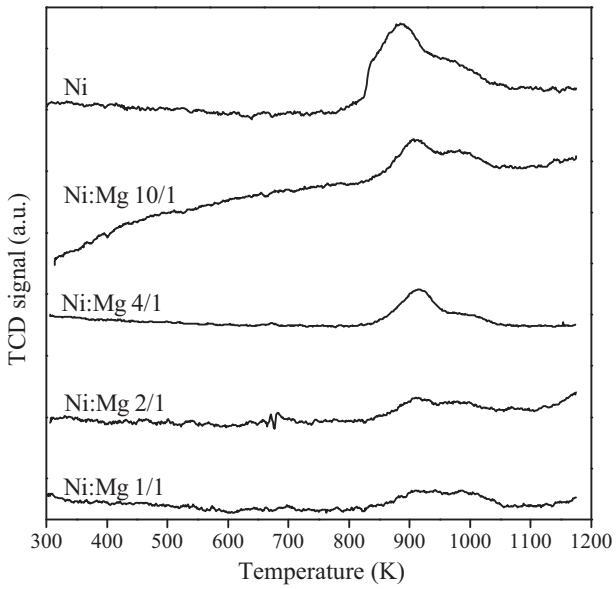

Fig. 8. TPO profiles after reaction for Mg promoted and Ni/β-SiC catalysts.

due to the decrease in metal particle size and the increase in the interaction between Ni and Mg in the resulting catalysts. The lower coke formation was found for catalysts Ni:Mg = 2/1 and Ni:Mg = 1/1. These two catalysts contained a similar quantity of coke, which would indicate that the addition of Mg decreased the coke generation rate until a given value of Ni:Mg molar ratio. Two peaks with maxima around 900 and 1000 K, which corresponds to the occurrence of two coke species, are observed in Fig. 8. The oxidation temperature of these peaks matches with that reported by Zhang et al. [43] for C_β and C_γ coke species. The former would be related with the generation of CO at high reaction temperatures and the later would be responsible of the catalyst deactivation. Our results show that the addition of Mg decreased the quantity of both coke species, leading to an increase of the catalyst stability. In addition, the Ni particle size in the catalysts used, measured by XRD analysis (Table 2), did not change in a meaningful way, concluding that no Ni sintering occurred during the reaction.

4. Conclusions

Alkaline and alkaline earth metals have been studied as cocations in Ni/β-SiC catalysts for methane tri-reforming. It was found that Na and K, despite their good properties as catalytic promoters in other reforming processes, were not useful for this process. It was due to their ability to increase the β-SiC oxidation rate during the calcination step, generating α-cristobalite and decreasing the surface area of the support. High loads of Ca also affected the final oxidation rate of the β-SiC catalyst.

Catalysts modified with Mg or with low load of Ca were tested in tri-reforming experiments. The presence of Mg enhanced both activity and stability of the catalyst, decreasing Ni metal particle size and increasing its basicity. It was observed that an increase in Mg loading favoured the formation of Ni metal particles smaller in diameter and decreased the reducibility of Ni, shifting the reduction peaks towards higher temperatures, likely due to the formation of a NiO-MgO solid solution. Catalytic activity was also analyzed in terms of Mg loading. A higher H_2/CO molar ratio and a better stability were observed for those catalysts with a higher amount in Mg. The stronger the basic sites in the catalyst, the higher the H_2/CO molar ratio was. Finally, the higher the interaction between Ni and Mg, the slower the catalyst deactivation rate was observed.

Acknowledgements

The authors would like to thank the Consejería de Ciencia y Tecnología of the Junta de Comunidades de Castilla-La Mancha (Project PPII10-0045-5875) and the Spanish government (grant FPU AP2009-2948) for their financial support.

References

[1] E. Iglesia, Applied Catalysis A: General 161 (1997) 59–78.
[2] M.E. Dry, Catalysis Today 71 (2002) 227–241.
[3] S.H. Lee, W. Cho, W.S. Ju, B.H. Cho, Y.C. Lee, Y.S. Baek, Catalysis Today 87 (2003) 133–137.
[4] M.A. Peña, J.P. Gómez, J.L.G. Fierro, Applied Catalysis A: General 144 (1996) 7–57.
[5] A.P.E. York, T. Xiao, M.L.H. Green, Topics in Catalysis 22 (2003) 345–358.
[6] M. Akiyama, Y. Oki, M. Nagai, Catalysis Today 181 (2012) 4–13.
[7] Y.J.O. Asencios, C.B. Rodella, E.M. Assaf, Applied Catalysis B: Environmental 132–133 (2013) 1–12.
[8] H.t. Jiang, H.q. Li, Y. Zhang, Ranliao Huaxue Xuebao 35 (2007) 72–78.
[9] D.L. Nguyen, P. Leroi, M.J. Ledoux, C. Pham-Huu, Catalysis Today 141 (2009) 393–396.
[10] F. Basile, P.D. Gallo, G. Fornasaria, D. Gary, V. Rosetti, A. Vaccari, Studies in Surface Science and Catalysis 167 (2007) 313–318.
[11] H. Liu, S. Li, S. Zhang, J. Wang, G. Zhou, L. Chen, X. Wang, Catalysis Communications 9 (2008) 51–54.
[12] E. Kockrick, L. Borchardt, C. Schrage, C. Gaudillere, C. Ziegler, T. Freudenberg, D. Farrusseng, A. Eychmüller, S. Kaskel, Chemistry of Materials 23 (2011) 57–66.
[13] J.M. García-Vargas, J.L. Valverde, A. De Lucas-Consuegra, B. Gómez-Monedero, P. Sánchez, F. Dorado, Applied Catalysis A: General 431–432 (2012) 49–56.
[14] J.M. García-Vargas, J.L. Valverde, A. de Lucas-Consuegra, B. Gómez-Monedero, F. Dorado, P. Sánchez, International Journal of Hydrogen Energy 38 (2013) 4524–4532.
[15] J. Juan-Juan, M.C. Román-Martínez, M.J. Illán-Gómez, Applied Catalysis A: General 301 (2006) 9–15.
[16] A. Casanovas, M. Roig, C. de Leitenburg, A. Trovarelli, J. Llorca, International Journal of Hydrogen Energy 35 (2010) 7690–7698.
[17] O. Yamazaki, T. Nozaki, K. Omata, K. Fujimoto, Chemistry Letters 21 (1992) 1953–1954.
[18] Z.L. Zhang, X.E. Verykios, Catalysis Today 21 (1994) 589–595.
[19] T. Horiuchi, K. Sakuma, T. Fukui, Y. Kubo, T. Osaki, T. Mori, Applied Catalysis A: General 144 (1996) 111–120.
[20] G.J. Kim, D.S. Cho, K.H. Kim, J.H. Kim, Catalysis Letters 28 (1994) 41–52.
[21] S.B. Tang, F.L. Qiu, S.J. Lu, Catalysis Today 24 (1995) 253–255.
[22] C. Song, Chemical Innovation 31 (2001) 21–26.
[23] C. Song, W. Pan, Catalysis Today 98 (2004) 463–484.
[24] V. Pareek, D.A. Shores, Journal of the American Ceramic Society 74 (1991) 556–563.
[25] F.L. Riley, The corrosion of ceramics: Where do we go from here? Key Engineering Materials 113 (1996) 1–14.
[26] K.N. Lee, R.A. Miller, Surface and Coatings Technology 86–87 (Part 1) (1996) 142–148.
[27] M.J.-F. Guinel, M.G. Norton, Journal of Materials Research 21 (2006) 2550–2563.
[28] A. Palermo, J.P.H. Vazquez, A.F. Lee, M.S. Tikhov, R.M. Lambert, Journal of Catalysis 177 (1998) 259–266.
[29] N.S. Jacobson, Journal of the American Ceramic Society 76 (1993) 3–28.
[30] Y.P. Tulenin, M.Y. Sinev, V.V. Savkin, V.N. Korchak, Catalysis Today 91–92 (2004) 155–159.
[31] B. Mile, D. Stirling, M.A. Zammitt, A. Lovell, M. Webb, Journal of Catalysis 114 (1988) 217–229.
[32] V.R. Choudhary, B.S. Uphade, A.S. Mamman, Journal of Catalysis 172 (1997) 281–293.
[33] A. Parmaliana, F. Arena, F. Frusteri, N. Giordano, Journal of the Chemical Society, Faraday Transactions 86 (1990) 2663–2669.
[34] A.H. Clemens, L.F. Damiano, T.W. Matheson, Fuel 77 (1998) 1017–1020.
[35] Z. Zhang, M. Baerns, Applied Catalysis 75 (1991) 299–310.
[36] M.C.J. Bradford, M.A. Vannice, Applied Catalysis A: General 142 (1996) 73–96.
[37] R.A.T.P.K. Flinn, Engineering Materials and Their Applications, Wiley, New York, Chichester, 1995.
[38] V.E.C.P.A. Henrich, The Surface Science of Metal Oxides, Cambridge University Press, Cambridge, New York, 1994.
[39] Y.-H. Wang, H.-M. Liu, B.-Q. Xu, Journal of Molecular Catalysis A: Chemical 299 (2009) 44–52.
[40] F. Arena, F. Frusteri, A. Parmaliana, L. Plyasova, A.N. Shmakov, Journal of the Chemical Society, Faraday Transactions 92 (1996) 469–471.
[41] L. Pino, A. Vita, F. Cipitì, M. Laganà, V. Recupero, Applied Catalysis B: Environmental 104 (2011) 64–73.
[42] S.H. Kim, S.-W. Nam, T.-H. Lim, H.-I. Lee, Applied Catalysis B: Environmental 81 (2008) 97–104.
[43] Z.L. Zhang, X.E. Verykios, Catalysis Today 21 (1994) 589–595.